CRITICAL SWITCHING CHARACTERISTICS OF THE SPIN-VALVE STRUCTURE IN THE ARBITRARY-DIRECTION MAGNETIC FIELD

© 2025 Iu. A. Iusipova

LLC «Alphachip», Moscow, Russia

**e-mail: linda_nike@mail.ru*

Received November 15, 2024

Revised December 14, 2024

Accepted December 30, 2024

Abstract. The dependences of the spin-valve critical switching field with planar and perpendicular anisotropy of layers on the anisotropy coefficient and the magnetic-field direction are analytically and numerically obtained. It is established that the smallest critical values of the field and switching time are achieved when the magnetic field deviates from the anisotropy axis by an angle of 45°.

Keywords: *spin valve, hard disk read head, magnetoresistive sensor, critical switching field*

DOI: 10.31857/S03676765250409e6

INTRODUCTION

Magnetic superlattices, such as spin valves, are actively used in microelectronics due to their versatility, scalability, and compatibility with K-MOS technologies [1]. Magnetoresistive random access memory (MRAM), hard magnetic disk drive (HMDD) read heads, and deterministic spin logic utilize spin valve switching between antiparallel and parallel states. HMDDs remain the most popular type of persistent storage due to their non-volatile nature, ease of fabrication, and high reliability [1]. In

turn, MRAM has all the advantages of HMDDs but with higher performance and integration, making it a potential replacement for other types of memory [2]. The principle of two possible outcomes is the basis of stochastic spin logic (PSL). The main advantages of spin logic devices include reversibility of processes, the ability to perform both deterministic and probabilistic computations, and data storage in a single integrated circuit [3]. The precession mode is applicable in spin-transfer nano-oscillators (STNOs). STNO generators provide extensive frequency and amplitude characteristics that can be varied by magnetic field and electric current [4]. The high sensitivity of spin valves to magnetic field and temperature has been utilized in various magnetic biosensors, magnetic field sensors and bolometric sensors. Arrays of spin-valve biosensors hold great promise in molecular diagnostics of cancer, infections and cardiovascular diseases [5]. In [6] the mechanism of operation of magnetoresistive LED as a magnetic field sensor is considered and it is shown that despite the small coefficient of giant magnetoresistance δ_{GMR}, it is possible to achieve a 100% change in the intensity of the emitted light, that is, to realize the operation of magnetoresistive LED in the "on or off" mode, respectively, in the presence or absence of a magnetic field. The analysis carried out in [7] showed that the sensitivity of spin-ventile structure to microwave irradiation along with the electrical contribution contains a thermal one, which makes it possible to use magnetic superlattices for detection and microwave visualization of objects at small distances.

All the above-mentioned emphasizes the relevance of research aimed at improving the energy efficiency and magnetic sensitivity of spin-gate structures. Nevertheless, one of the main problems of their application remains high energy

consumption during switching by means of a magnetic field [8 - 10]. In this work, the behavior of a spin-valve in a magnetic field of arbitrary orientation is examined with the goal of reducing energy consumption and increasing sensitivity without loss of fast performance. For this purpose the following tasks were set: to construct a macromagnetic model of a spin valve placed in a field with an arbitrary direction, by means of bifurcation analysis of the system of equations of the model to obtain equations for the coordinates of its special points, from these equations to derive formulas for the dependence of the critical switching fields on the direction of the magnetic field and to evaluate the values of speed and sensitivity of the spin valve on the basis of ten different materials.

The classical geometry of field switched MRAM cells and magnetic field sensors uses the field direction along the anisotropy axis [5]. As a method of energy reduction, it is proposed to add a perpendicular component to the magnetic field directed along the anisotropy axis. Although this modification will lead to a complication of the geometry of the structure, however, for the topology of integrated circuits it means adding only one additional power bus for the whole circuit. This is due to the fact that the additional field component can be applied simultaneously to the entire matrix of spin gates, which can serve as a clock signal for all cells [1]. At the same time, the value of this component will not be sufficient to switch the spin valve, and thus will not lead to errors in the operation of the device.

BASIC EQUATIONS

The object of study is a spin valve with a square cross section with side d_0= 11 nm [2], shown in Fig. 1. It consists of two ferromagnetic layers FM1 and FM2 separated by a non-magnetic NM interlayer of thickness $d_{(NM)\ (1)}$= 1.2 nm [11]. Two types of anisotropy of ferromagnetic layers were considered in the study: planar and perpendicular to the surface of the layers. The antiferromagnetic layer AF is used to anchor the direction of the magnetization vector $\vec{M}_1$ in the thicker (fixed) ferromagnetic layer FM1, whose thickness $d_{(FM)\ (1)}$= 5 nm [2]. The resistance of the superlattice depends on the direction of the magnetization vector $\vec{M}_2$ in the thin (free) layer FM2, whose thickness is $d_{(FM)\ (2)}$= 2 nm [2]. The structure is placed in the magnetic field $\vec{H}$, whose direction is given by the azimuthal angle φ and zenith angle θ. The magnetization vector of the free layer $\vec{M}_2$ can change its direction, M_X, M_Y, M_Z are its projections on the corresponding *OX*, *OY*, *OZ* axes. An electric current of density *J* is passed perpendicular to the plane of the layers opposite to the *OZ* axis.

The spin valve has two main stationary states: parallel with resistance R_{P} and antiparallel with resistance R_{AP}. They can be expressed through the specific resistances of the ferromagnetic ρ_{F} and the spin polarization parameter *P* [1]. The total resistance of a magnetic superlattice for any position of the vector $\vec{M}_2$ is described by the expression R= 0.5 [(R_{P}+ $R_{(\text{AP})}$)+ (R_{P}- R_{AP})(M_i/ M_s)], where $M_{(i)}$ is the projection of the vector $\vec{M}_2$ on the anisotropy axis, and M_s is the saturation magnetization.

The dynamics of the vector $\vec{M}_2$ is described by the phenomenological Landau-Lifshitz-Hilbert equation

$$\frac{\partial \vec{M}_2}{\partial t} = -|\gamma|\mu_0 \left[\vec{M}_2 \times \vec{H}_{\text{эфф}}\right] + \frac{\alpha}{M_{\text{s}}}\left[\vec{M}_2 \times \frac{\partial \vec{M}_2}{\partial t}\right], \qquad (1)$$

where α is the dissipation coefficient,$\vec{H}_{эфф}$ is the effective magnetic field including the following components:

– light-axis anisotropy field equal to $2M_XK / (M_{(s)}{}^{2)}\mu_0)$ for the direction along the *OX* axis (planar anisotropy) and $2M_ZK / (M_{(s)}{}^{2)}\mu_0)$ for the direction along the *OZ* axis (perpendicular anisotropy), where *K is the* first anisotropy constant;

– demagnetization field equal to M_Z;

– field due to the spin-polarized current contribution, according to [8 - 10], is of the form $GJ\hbar / (ed_{(FM)(2)}\mu_{(0)}M_{(s)}{}^{2)})\ [(\vec{M}_1 / M_s)\times\vec{M}_2\ ]$, where $G= c / (b+ M_X/ M_s)$ is the current coefficient, here $c= 4P^{(3/2)}/ (1+P)^3$, $b= 3 - 4c$ [8 - 10];

– external magnetic field .$\vec{H}$

The influence of the antiferromagnetic AF layer is accounted for in the effective field$\vec{H}_{эфф}$ only for the magnetization vector of the fixed layer$\vec{M}_1$ such that the vector vector$\vec{M}_1$ has a fixed direction and magnitude.

The following constants are used in the calculations: $\mu_0$is the magnetic constant, γ is the gyromagnetic ratio, $\hbar$ is Planck's constant, and *e* is the elementary electric charge.

The following six magnetically soft materials were selected as the materials for layers FM1 and FM2:

– cobalt and iron, whose monocrystalline films are easier and cheaper to obtain;

– $Fe_{70}Co_{(30)}$ (permendur) and $Fe_{(60)}Co_{(20)}$ B20with high spin polarization parameter $P >$ 0.5;

– $Co_{93}Gd_7$and $Co_{80}Gd_{20}$, having the best magnetic properties to reduce the magnetic switching field.

The following magnetically hard alloys have also been used:

– $Co_{50}Pt_{50}$with small saturation magnetization M_s;

– $Fe_{50}Pd_{50}$and $Fe_{(50)}Ni_{(50)}$ (permalloy) are ferromagnetic alloys with a small dissipation factor $\alpha = 0.01$;

– $Fe_{50}Pt_{50}$is the alloy with the highest anisotropy constant.

The materials are classified into magnetically soft and magnetically hard materials taking into account the magnetically hardness criterion $\kappa = (K / (M_{(s)}{}^{2)} \mu_{(0)}))^{1/2}$. Magnetically hard materials have the criterion $\kappa > 1$ [12]. The parameters of these ferromagnetics are summarized in Table 1. Copper was chosen as the material for the non-magnetic interlayer. Defects in the microstructure and the degree of structural order of materials are not taken into account in the model under consideration.

BIFURCATION ANALYSIS

The most important characteristic of the dynamics of any vector are its equilibrium positions, or, in another way, the special points of the system of equations. In papers [8 - 10], an effective method for finding the number and coordinates of the equilibrium positions of the free layer magnetization vector of the spin fan $\vec{M}_2$. Equations (P1) and (P2) for calculating the coordinates of the special points of the system (1) for planar and perpendicular anisotropy, respectively, are presented in the Appendix.

The type of special points is determined using the Cauchy theorem on the existence or uniqueness of the solution of the system of differential equations, which is not fulfilled in them. For this purpose, the eigenvalues of the Jacobi matrix of the system (1) are calculated. Depending on the signs of their real parts, the stability of the singular point is determined. While the magnitude of the imaginary part of the eigenvalues of the Jacobi matrix determines the type of equilibrium position (focus, node, saddle).

By dividing the plane of control parameters H - J by a frequent grid and determining the number, coordinates, and type of special points in each node of this grid, bifurcation diagrams for equation (1) for different materials, anisotropy configurations, and magnetic field direction were constructed in [8 - 10].

When considering bifurcation diagrams, it was observed that the critical switching field of the spin valve $H_{min}$for planar anisotropy depends strongly and nonlinearly on the direction of the magnetic field, i.e., on the angles φ and θ [9], and for perpendicular anisotropy only on the angle θ [10], while being independent of the dissipation factor α. This is because equations (P1) and (P2) do not depend on α, and also equation (P2) does not depend on the angle φ. In [9] it was noted that for planar anisotropy the decrease of the angle θ leads to a monotonic increase of the critical switching field, so we will perform all further calculations for this direction of anisotropy for $\theta = \pi / 2$.

In order to numerically obtain the dependence of $H_{min}(\varphi, \theta)$, bifurcation diagrams at zero current *(*J= 0) (Fig. 2) for a cobalt-based spin valve with planar anisotropy in the φ - H plane ($\theta = \pi / 2$) (Fig. *2a*) and for $Fe_{50}Pt_{50}$with perpendicular anisotropy for θ

- H (Fig. *2b*). They highlight regions with qualitatively different dynamics of the magnetization vector$\vec{M}_2$. In regions I and VI, there can be no spin fan switching, since both ground steady states are stable. In regions II and IV, switching to the parallel state is observed, and in regions III and V - to the antiparallel state. It is worth noting that system (1) has 6 special points in region I, 4 special points in regions II, III and VI, and 2 special points in regions IV and V. The number of special points determines the type of dynamics of the magnetization vector of the free layer of the spin fan. The more special points, the more complex the trajectory of the end of the vector$\vec{M}_2$, which leads to a greater number of oscillations in the graph of the transient switching process of the spin valve. Oscillations in the transient can lead to errors in the operation of the integrated circuit, so it is necessary to choose modes of operation of the spin valve in regions with fewer special points.

The bifurcation lines bounding regions I and VI are highlighted in red - these are the stability lines of the special points of the system (1) corresponding to the parallel and antiparallel states of the spin fan. They numerically determine the dependence of the critical switching field $H_{\min}$on the angle φ or θ. The appearance of these bifurcation lines suggests that the functions $H_{(\min)}(k, \varphi)$ and $H_{(\min)}(k, \theta)$ have a single minimum. These lines also correspond to the bifurcation of the vanishing of a pair of special points, that is, the pair of real roots of equations (P1) and (P2) goes to the region of complex numbers. Applying to them the criteria for the loss of stability of stationary states of the spin fan (the real part of the eigenstates of the linearization matrix for a given point is 0), as well as the criterion $M_{(X)}, M_Y, M_Z \in \mathbb{R}$ in the course of this study, independently of each other for planar and perpendicular anisotropy, taking into

account J= 0, the formula for calculating the critical switching field normalized to the saturation magnetization was analytically obtained (2).

$$H_{\min}/ M_s = \pm\ N((q^2 + sq + s^2 - 1) / q)^{(1/2)}, \quad (2)$$

where q= (0.5 (s - 1) ((4s+ 5)$^{1/2}$+ 2s+ 2$s^{(2)-1}$))$^{(1/3)}$, for planar anisotropy at θ = π / 2 the multipliers N and s take the following values: N= k , s= 9cos^4 φ - 9cos^2 φ+ 1. For perpendicular anisotropy at any φ, the coefficients N and s are k - 1 and 9cos^4 θ - 9cos^2 θ+ 1, respectively. The anisotropy field coefficient k is calculated using the anisotropy constant K and the saturation magnetization $k = 2K / (M_s^2 \mu_0)$.

Fig. 3 shows the corresponding plots of the dependence of $H_{(\min)}(k, \varphi)$ and $H_{(\min)}(k, \theta)$ for planar and perpendicular anisotropy. It is worth noting that the cross sections of the surfaces$_{H(\min)}(k, \varphi)$ and $H_{(\min)}(k, \theta)$ in Fig. 3 respectively by the planes (φ - $H_{\min}$) and (θ - $H_{\min}$) coincide with the corresponding numerically obtained bifurcation lines in the diagrams of Fig. 2.

Differentiating equation (2) for planar anisotropy by the angle φ, and for perpendicular anisotropy by the angle θ, and equating the derivative to zero, we obtain that the function (2) in both cases has a single minimum in the coordinate $(N/2, \pi/4)$. For planar anisotropy, the minimum value$_{H(\min)}$/ M_s is half k when θ = π/2, φ = π/4, and for perpendicular anisotropy it is (k - 1)/2 when θ = π / 4, which is half the critical switching field when the magnetic field is directed along the anisotropy axis. These results coincide with the numerical values obtained by constructing bifurcation diagrams (Fig. 2). This means a twofold reduction in the energy consumption of the spin valve as a magnetic field switched MRAM memory cell [5]. Table 2 shows the

calculated critical switching fields of the spin valve when the field is directed along the anisotropy axis and when it is deflected from it by 45°.

NUMERICAL RESULTS

At switching of the spin valve in the field not parallel to the anisotropy axis, the stable special point, to which the switching occurs, is shifted relative to the basic stationary equilibrium state. Thus switching will occur in two steps. First, in a magnetic field, the vector$\vec{M}_2$ will switch to a stable special point near one of the stationary states (parallel or antiparallel), and then, when the magnetic field is turned off, the end$\vec{M}_2$ will switch to the stationary state in the basin of attraction. Thus, the switching of the spin valve in a magnetic field not parallel to the anisotropy axis will be two-cycle.

Table 2 shows estimates of the switching time t for the first switching cycle of the spin valve in a magnetic field close to the critical field, made by modeling the switching of the spin valve using the Runge-Kutta method of the fourth order. The data in Table 2 show that for almost all materials the switching time is lower for a field deflected from the anisotropy axis by an angle of π/4. The corresponding cells are shaded in gray.

The sensitivity of the spin valve as a magnetic field sensor $S_0$is inversely proportional to the magnetic field change $S_0 = dR/dH$ [5]. However, the shift of the stable equilibrium position from the stationary one reduces the change in resistance dR, which in turn reduces the sensitivity S_0. The numerical experiments performed for ten considered materials to simulate the dynamics of the spin valve in a magnetic field deviated from the anisotropy axis showed that at a field magnitude close to the critical

one, the deviation of the singular point from the stationary state is not more than 10%. Thus, the reduction of S_0due to reduction of dR, in this case, will not be more than 10%, but a 2-fold reduction of the switching field will make a greater contribution to the change in the value of S_0, as can be seen from the data presented in Table 2.

From the results of numerical calculations given in Table 2 it can be concluded that the smallest critical switching field has $Co_{93}Gd_7$with planar anisotropy at $\theta = \pi/2$, $\varphi = \pi/4$. Accordingly, the $Co_{93}Gd_7$alloy has the highest sensitivity of 89.08 Ohm/Tl.

The lowest switching time of 1 ns is observed for $Co_{50}Pt_{(50)}$and $Fe_{(50)}Pt_{(50)}$, but the critical switching field for these materials is~ 700 times higher than that of $Co_{93}Gd_7$. The optimal material for these two parameters is the $Fe_{70}Co_{30}$permendur with planar anisotropy, since it has a critical switching field of 0.015 MA/m ($\theta = \pi/2$, $\varphi = \pi/4$) at a switching time of 3 ns.

CONCLUSION

Thus, the dependence of the critical switching field of the spin fan H_{min}on its direction is numerically and analytically obtained. Studies have been carried out for ten different ferromagnetics with planar and perpendicular anisotropy. It is determined that the deviation of the magnetic field by an angle of 45° from the anisotropy axis reduces the critical switching field $H_{min}$by two times and increases the speed of the spin valve for most of the considered materials. It is shown that the decrease in sensitivity due to the deviation of the magnetic field from the anisotropy axis is completely leveled by its growth due to a twofold decrease in H_{min}. Numerical calculations of sensitivity and switching time have shown that the best of the considered ferromagnetics for

fabrication of magnetoresistive sensors and reading heads of hard disks is $Co_{93}Gd_7$with planar anisotropy of layers, while for magnetoresistive MRAM cells switched by magnetic field, the optimal material is permendur ($Fe_{70}Co_{30)}$. For both applications, the best magnetic field direction will be at an angle of $\pi/4$ to the anisotropy field.

APPENDIX. DETERMINATION OF COORDINATES OF SPECIAL POINTS FOR THE LANDAU-LIFSHITZ-HILBERT SYSTEM

1. For the case of planar anisotropy and arbitrary magnetic field direction (θ, φ - any), let us write the system of equations (1) in coordinate form.

$$dm_x / d\tau = P(m_x, m_y, m_z) = m_y m_z + h(v m_z - w m_y) - Gj(m_y^2 + m_z^2) +$$
$$+ \alpha(k m_x + m_x m_z^2 - k m_x^3) + \alpha h(u - u m_x^2 - v m_x m_y - w m_x m_z),$$
$$dm_y / d\tau = Q(m_x, m_y, m_z) = - m_x m_z (k + 1) + h(w m_x - u m_z) - Gj(\alpha m_z - m_x m_y) +$$
$$+ \alpha(m_y m_z^2 - k m_x^2 m_y) + \alpha h(v - v m_y^2 - u m_x m_y - w m_y m_z),$$
$$dm_z / d\tau = S(m_x, m_y, m_z) = k m_x m_y + h(u m_y - v m_x) + Gj(\alpha m_y - m_x m_z) +$$
$$+ \alpha(m_z^3 - m_z - k m_x^2 m_z) + \alpha h(w - w m_z^2 - u m_x m_z - v m_y m_z).$$

Here $\tau = t\gamma\mu_0 M_s / (1 + \alpha^2)$, $u = \sin\theta \cdot \cos\varphi$, $v = \sin\theta \cdot \sin\varphi$, $w = \cos\theta$, $h = H / M_s$, $j = J\hbar / (e d_{FM2} \mu_0 M_s^2)$, $m_x = M_X / M_S$, $m_y = M_Y / M_S$, $m_z = M_Z / M_S$, $k = 2K / (M_s^2 \mu_0)$.

To find the equilibrium positions of the system (1), equate its right-hand sides to zero and, by successive elimination of variables, obtain the equation for calculating the component m_x:

$$\sum_{f=0}^{10} A_f m_x^f = 0, \qquad (\Pi 1)$$

where

$A_{10} = k^2 (k + 1)^2$,

$A_9 = 2(k + 1)\, k\, (2bk\, (k + 1) + hu\, (2k + 1))$,

$A_8 = ((k + 1)\, (hu\, (hu\, (5k + 1) + 8bk\, (2k + 1)) + h^2 v^2 + 2j^2 c^2 k) + (k + 1)^2\, (6b^2 k^2 - k^2) +$

$+ h^2 k\, (k + v^2))$,

$A_7 = 2\,(2\,(b^3k^2 - k^2b + h^2b + 6hb^2uk - huk)\,(k+1)^2 + (k+1)\,(k\,(hu\,(10hbu + 1 - 6b^2) +$

$+ 2j^2c^2b) - 2h^2bw^2 + c^2j^2hu + h^3u) + h\,(-2hk\,(u^2 + w^2)\,b + uk\,(j^2c^2 + u^2h^2) -$

$- hw\,(huw + jcv))),$

$A_6 = ((k+1)^2\,((b^4 - 6b^2)\,k^2 + k\,(16hbu\,(b^2 - 1)) + 6h^2b^2) + (k+1)\,(2khu\,(3hu\,(5b^2 -$

$- 1) - 4b\,(b^2 - 1)) + 2kc^2j^2\,(b^2 - 1) + 8hbu\,(h^2u^2 + c^2j^2 + h^2) + 6h^2b^2\,(v^2 - w^2 - 1)) +$

$+ (j^4c^4 + hj^2c^2\,(h + hu^2 - 4bu) - 6h^2bjvwc + h^2(\,u^2\,(h^2 - 1) + 2b\,(v^2 - 1)\,(4hu - 3b)))),$

$A_5 = 2\,(2b^2\,(k+1)^2\,(h^2b - bk^2 - 6hku + hb^2ku) + (k+1)\,(kb\,(2u^2h^2\,(5b^2 - 6) -$

$- buh\,(b^2 - 6) - 2c^2j^2) + (6h^3b^2u)) - (2k+1)\,h\,(h\,(hu^3 + 2b^3w^2) - c^2j^2u\,(b^2 - 1)) +$

$+ h^2b\,(2kbu^2(3hu - b\,) + (2hu\,(hu - 3bw^2) + c^2j^2(u^2 + 1) - 2u^2 - 3bvcjw))),$

$A_4 = (-b^3k\,(bk + 8hu)\,(k+1)^2 + b\,(k+1)\,(h^2b^3(v^2 + k + 5ku^2) + 8hub^2\,(u^2h^2 - k^2) -$

$- 2kb(j^2c^2 + 18u^2h^2) - 4hu\,(j^2c^2 + 2u^2h^2)) + h^2b^4\,(u^2 - w^2k) + 2h^2b^3\,(4khu - vwcj +$

$+ 4huv^2) + h^2b^2\,(j^2c^2(u^2 + 1) + 6u^2\,(h^2 - 1)) - 4khub\,(j^2c^2 + 2u^2h^2) - (j^2c^2 + u^2h^2)^2),$

$A_3 = 2hbu\,(((-2k^2 + u^2h^2)b^2 - 12hubk - 5u^2h^2)\,b\,(k+1) - b^3\,(k+1)^2 - (j^2c^2 - b^2 +$

$+ u^2h^2)\,(2hu + 2bk + b) + b\,((h^2k - k + h^2v^2)b^2 + 2hub\,(h^2 - 2) - 5u^2h^2k)),$

$A_2 = -h^2u^2b^2\,(6b^2k\,(k+1) + 8hbu\,(2k+1) + 2j^2c^2 - h^2b^2 + b^2 + 6u^2h^2),$

$A_1 = -2h^3u^3b^3\,(2hu + 2bk + b),$

$A_0 = -h^4b^4u^4.$

The remaining coordinates are calculated from the equations S and P by substituting the values obtained from equation (P1).

2. For the case of perpendicular anisotropy and arbitrary magnetic field direction (θ, φ - any), let us write the system of equations (1) in coordinate form.

$$dm_x / d\tau = P(m_x, m_y, m_z) = -m_ym_z\,(k-1) + h(vm_z - wm_y) - Gj(m_xm_z + \alpha m_y) +$$

$$+ \alpha(m_xm_z^2 - km_xm_z^2) + \alpha h(u - vm_xm_y - wm_xm_z - um_x^2\,),$$

$$dm_y / d\tau = Q(m_x, m_y, m_z) = m_x m_z(k-1) + h(wm_x - um_z) - Gj(\alpha m_x - m_y m_z) +$$

$$+ \alpha(m_y m_z^2 - k m_x^2 m_z) + \alpha h(v - u m_x m_y - v m_y^2 - w m_y m_z),$$

$$dm_z / d\tau = S(m_x, m_y, m_z) = k m_x m_y + h(u m_y - v m_x) - Gj(m_y^2 + m_x^2) +$$

$$- \alpha(m_z^3 - m_z)(k-1) + \alpha h(w - u m_x m_z - w m_z^2 - v m_y m_z).$$

To find the equilibrium positions of the system (1), we should equate its right-hand sides to zero and by successively excluding variables we obtain the equation for calculating the component m_z. Then, by successively excluding variables, we obtain the expression (P2) for calculating the coordinate $m_z$of special points:

$$\sum_{f=0}^{10} B_f m_z^f = 0, \qquad (\Pi 2)$$

where

$B_6 = (k-1)^2$,

$B_5 = 2\,(hw - b + bk)(k-1)$,

$B_4 = 2k - 4hbw + 4hbwk + h^2 + b^2 - k^2 - 2b^2k + b^2k^2 + c^2j^2 - 1$,

$B_3 = 2(hw - b + 2bk - hkw + h^2b - bk^2 - hwb^2 + hkwb^2)$,

$B_2 = 4hbw - 4hbkw - b^2 + 2kb^2 - h^2w^2 - b^2k^2 - c^2j^2 + h^2b^2$,

$B_1 = -\,2hbw(hw - b + bk)$,

$B_0 = -\,h^2b^2w^2$.

It should be noted that expression (3) is independent of the parameters u and v, which means that the coordinates of the special points along the OZ axis do not depend on the azimuthal angle φ. For non-zero fields and currents at $w = 1$, equation (P2) has two significant roots $m_z = \pm 1$, and for $H = 0$, $J = 0$, three roots $m_z = \pm 1$ and $m_z = 0$. In the

case of $w \neq 1$, expression (P2) has two or four real roots whose modulus is less than one.

REFERENCES

1. *Iusipova Iu.A., Popov A.I. //* Semiconductors. 2021. V. 55. No. 13. P. 1008.

2. *Nowak J.J., Robertazzi R.P., Sun J.Z. et al.* // IEEE Magn. Lett. 2016. V. 7. Art. No. 3102604.

3. *López A., Costa J.D., Grollier J. et al.* // Phys. Rev. Appl. 2024. V. 22. Art. No. 014082.

4. *You Ch.Y.* // J. Magn. 2009. V. 14. No. 4. P. 168.

5. *Tsymbal E.Y., Žutić I.* Handbook of spin transport and magnetism. Boca Raton: CRC Press Taylor & Francis Group, 2012. 777 p.

6. *Ved M., Danilov Y., Demina P. et al.* // Appl. Phys. Lett. 2021. V. 118. Art. No. 092402.

7. *Demin G.D., Zvezdin K.A., Popkov A.F.* // Adv. Cond. Mater. Phys. 2019. No. 1. Art. No. 5109765.

8. *Ostrovskaya N.V., Iusipova Iu.A //* Phys. Met. Metallogr. 2019. V. 120. No. 13. P. 1291.

9. *Iusipova Iu.A., Skidanov V.A.* // Bull. Russ. Acad. Sci. Phys. 2023. V. 87. No. 3. P. 310.

10. *Iusipova Iu.A*. // IEEE Magn. Lett. 2022. V. 13. Art. No. 4501605.

11. *Shalygina E.E., Makarov A.V., Kharlamova A.M.* // Proc. of the Nanomeeting-2017: Physics, chemistry and application of nanostructures (Minsk, 2017). P. 89.

12. *Skomski R., Coey J.M.D.* // Scripta Materialia. 2016. V. 112. No. 2. P. 3.

13. *Skomski R*. Simple Models of Magnetism. NY: Oxford university press, 2008. 335 p.

14. *Kawai T., Asai Y., Ohtake M. et al.* // EPJ Web Conf. 2013. V. 40. Art. No. 13001.

15. *Moodera J.S., Kim T.H., Tanaka C. et al.* // Phil. Mag. B. 2000. V. 80. No. 2. P. 195.

16. *Babichev A.P., Babushkina N.A., Bratkovsky A.M. et al.* Physical quantities: Reference book. Moscow: Energoatomizdat, 1991. 1232 c.

17. *Huang S.X., Chen T.Y., Chien C.L.* // Appl. Phys. Lett. 2008. V. 92. Art. No. 242509.

18. *Nguyen M.H., Pai C.F., Nguyen K.X. et al.* // Appl. Phys. Lett. 2015. V. 106. Art. No. 222402.

19. *Ikeda S., Miura K., Yamamoto H. et al.* // Nature Mater. 2010. V. 9. P. 721.

20. *Kaiser C., PapWorth Parkin S.S.* // US Patent № US007230265B2. 2007.

21. *Papusoi C., Le T., Lo C.C.H. et al.* // J. Physics D. 2018. V. 51. No 32. Art. No. 325002.

22. *Kawai T., Itabashi A., Ohtake M. et al.* // EPJ Web Conf. 2014. V. 75. Art. No. 02002.

23. *Seemann K.M., Hickey M.C., Baltz V. et al.* // New J. Phys. 2010. V. 12. Art. No. 033033.

24. *Seki T., Mitani S., Yakushiji K. et al.* // Appl. Phys. Lett. 2006. V. 88. Art. No. 172504.

25. *Ogiwara M., Iihama S., Seki T. et al.* // Appl. Phys. Lett. 2013. V. 103. Art. No. 242409.

26. *Guslienko K.Y., Aranda G.R., Gonzalez J. et al.* // J. Phys. Conf. Ser. 2011. V. 292. Art. No. 012006.

FIGURE CAPTIONS

Figure 1: Geometry of the spin valve model.

Figure 2: Bifurcation diagrams at zero current in the H - φ plane for cobalt with planar anisotropy at $\theta = \pi/2$ (a) and in the H - θ plane for $Fe_{50}Pt_{50}$with perpendicular anisotropy (b).

Figure 3: Dependence of the critical switching field on its direction for planar (a) and perpendicular anisotropy (b).

Table 1. Material parameters used in the calculations.

Material		$\mu_0 M_s$, Tl	α	K, kJ/m^3	P	ρ_F, nOm·m	R_{AP}, Ohm	R_P, Ohm	δ_{GMR}, %
Magnetically soft	Co [13]	1.76	0.020	530	0.35	62.4	4.11	3.70	11
	Fe [13, 14]	2.15	0.008	48	0.40	97.1	6.58	5.71	15
	$Fe_{70}Co_{30}$ [14 – 16]	2.40	0.015	35	0.55	83.3	6.62	4.93	34
	$Fe_{60}Co_{20}B_{20}$ [17 – 19]	1.96	0.040	210	0.53	195.6	15.01	11.42	31
	$Co_{93}Gd_7$ [20]	1.21	0.020	1.88	0.30	78.1	4.96	4.61	8

	$Co_{80}Gd_{20}$ [20]	0.10	0.020	1.38	0.10	112.9	6.67	6.62	1
Magnetically hard	$Co_{50}Pt_{50}$ [13, 21]	1.01	0.030	4900	0.30	100.2	6.35	5.88	8
	$Fe_{50}Pd_{50}$ [13, 22, 23]	1.37	0.010	1800	0.50	99.0	7.37	5.83	26
	$Fe_{50}Pt_{50}$ [13, 24]	1.43	0.050	6600	0.40	106.0	7.17	6.23	15
	$Fe_{50}Ni_{50}$ [25, 26]	1.59	0.010	1300	0.20	80.0	4.87	4.71	3

Table 2. Critical switching fields, switching times at these fields, and spin valve sensitivity calculated for different materials and magnetic field direction configurations.

Material	Planar anisotropy						Perpendicular anisotropy					
	$\theta = \pi / 2, \varphi = 0$			$\theta = \pi / 2, \varphi = \pi / 4$			$\theta = 0$			$\theta = \pi / 4$		
	H_{min}, MA/m	t, ns	S_0, Ohm/Tl	H_{min}, MA/m	t, ns	S_0, Ohm/Tl	H_{min}, MA/m	t, ns	S_0, Ohm/Tl	H_{min}, MA/m	t, ns	S_0, Ohm/Tl
Co	0.605	9	0.27	0.301	7	0.52	0.922	47	0.20	0.461	42	0.39
Fe	0.047	17	7.69	0.022	21	14.91	1.899	55	0.21	0.949	60	0.40
$Fe_{70}Co_{30}$	0.032	11	23.01	0.015	3	44.64	2.416	18	0.36	1.208	16	0.69
$Fe_{60}Co_{20}B_{20}$	0.218	7	6.66	0.107	4	12.93	1.425	29	1.06	0.712	25	2.06
$Co_{93}Gd_7$	0.013	12	45.92	0.007	8	89.08	1.003	84	0.15	0.501	73	0.29
$Co_{80}Gd_{20}$	0.028	442	0.77	0.014	135	1.49	0.069	464	0.41	0.034	126	0.79
$Co_{50}Pt_{50}$	9.645	5	0.02	4.851	1	0.04	9.347	17	0.02	4.673	10	0.04
$Fe_{50}Pd_{50}$	2.616	9	0.23	1.314	6	0.45	1.631	254	0.40	0.815	212	0.77
$Fe_{50}Pt_{50}$	9.126	4	0.04	4.610	1	0.08	8.179	49	0.05	4.089	24	0.09
$Fe_{50}Ni_{50}$	1.645	7	0.04	0.817	9	0.07	0.427	446	0.17	0.213	382	0.32

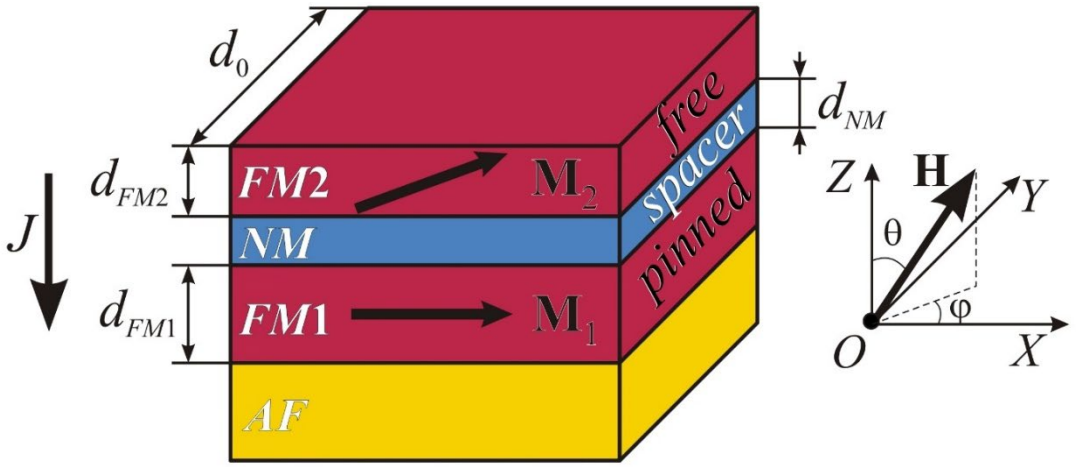
d_0
d_{FM2}
d_{FM1}
d_{NM}
J
FM2
NM
FM1
AF
M_2
M_1
free
spacer
pinned
Z
H
Y
θ
φ
O
X

Fig. 1.

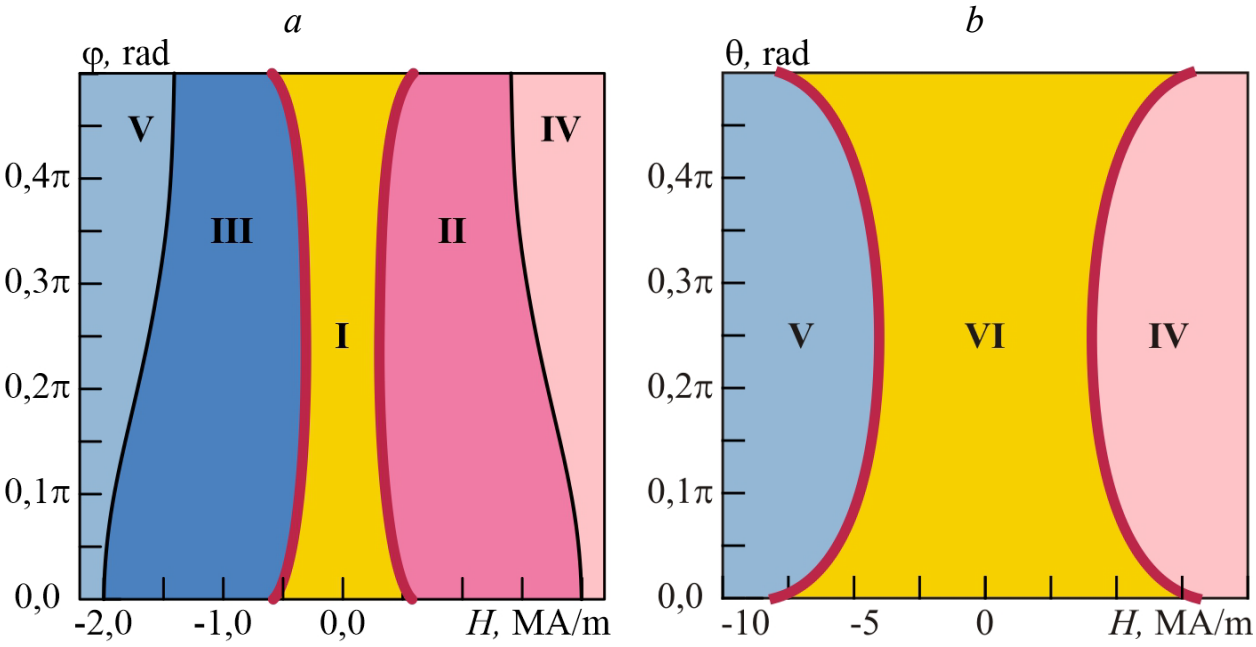
a
φ, rad
V
III
I
II
IV
0,4π
0,3π
0,2π
0,1π
0,0
-2,0
-1,0
0,0
H, MA/m
b
θ, rad
V
VI
IV
0,4π
0,3π
0,2π
0,1π
0,0
-10
-5
0
H, MA/m

Fig. 2.

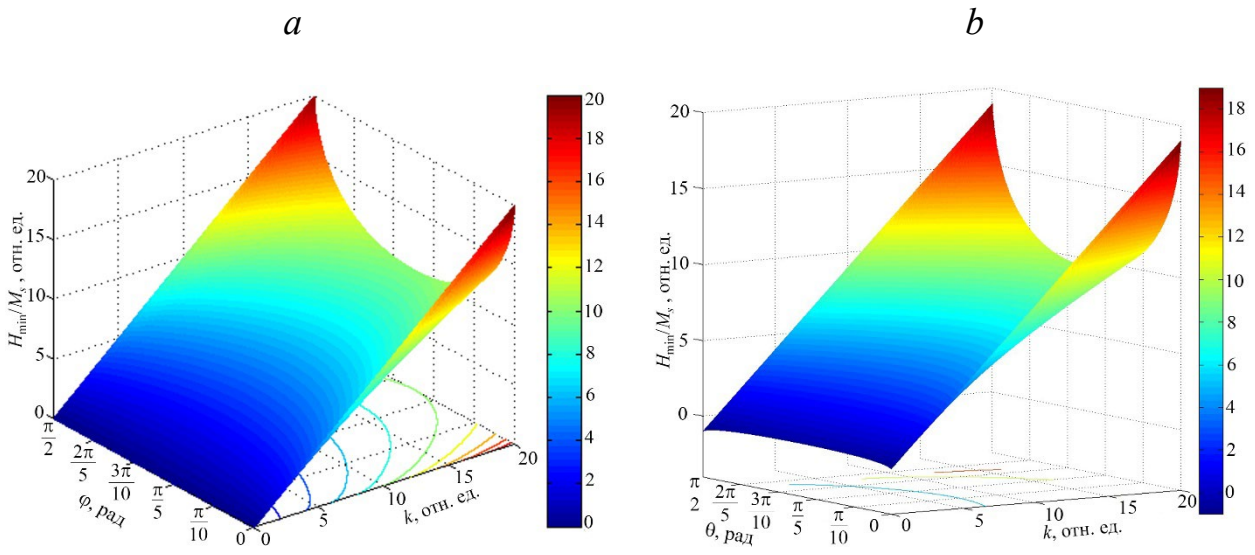

Fig. 3.